Human Movement Science 68 (2019) 102525

Contents lists available at ScienceDirect

Human Movement Science

journal homepage: www.elsevier.com/locate/humov

Visuomotor error augmentation affects mediolateral head and trunk stabilization during walking

Mu Qiao[a,*], Jackson T. Richards[b], Jason R. Franz[b]

[a] Department of Kinesiology, Louisiana Tech University, Ruston, LA, USA
[b] Joint Department of Biomedical Engineering, University of North Carolina at Chapel Hill, Chapel Hill, NC and North Carolina State University, Raleigh, NC, USA

ARTICLE INFO

Keywords:
Optical flow
Medio-lateral
Anchor
Adaptation
Stability

ABSTRACT

Prior work demonstrates that humans spontaneously synchronize their head and trunk kinematics to a broad range of driving frequencies of perceived mediolateral motion prescribed using optical flow. Using a closed-loop visuomotor error augmentation task in an immersive virtual environment, we sought to understand whether unifying visual with vestibular and somatosensory feedback is a control goal during human walking, at least in the context of head and trunk stabilization. We hypothesized that humans would minimize visual errors during walking – i.e., those between the visual perception of movement and actual movement of the trunk. We found that subjects did not minimize errors between the visual perception of movement and actual movement of the head and trunk. Rather, subjects increased mediolateral trunk range of motion in response to error-augmented optical flow with positive feedback gains. Our results are more consistent with our alternative hypothesis – that visual feedback can override other sensory modalities and independently compel adjustments in head and trunk position. Also, aftereffects following exposure to error-augmented optical flow included longer, narrower steps and reduced mediolateral postural sway, particularly in response to larger amplitude positive feedback gains. Our results allude to a recalibration of head and trunk stabilization toward more tightly regulated postural control following exposure to error-augmented visual feedback. Lasting reductions in mediolateral postural sway may have implications for using error-augmented optical flow to enhance the integrity of walking balance control through training, for example in older adults.

1. Introduction

Humans regulate lateral balance in walking through coordinated adjustments between the continuous control of posture (i.e., head and trunk stabilization) and the discrete (step-to-step) control of foot placement (i.e., step width). Here, successful coordination depends on appropriate motor planning and execution, which in turn depend on having accurate and reliable sensory feedback. Optical flow perturbations, a class of experimental paradigms used in the study of walking balance control, are unique in that they exclusively target that sensory feedback through the visual perception of lateral imbalance (O'Connor & Kuo, 2009; Qiao, Feld, & Franz, 2018). Somewhat surprisingly, walking balance is acutely susceptible to those perturbations, and the resulting motor responses may have the capacity to inform how sensory feedback is used in the planning and execution of stable locomotion. For example, head and trunk kinematics during walking spontaneously synchronize (i.e., entrain) to a broad range of driving frequencies of perceived

* Corresponding author at: Department of Kinesiology, Louisiana Tech University, P.O. Box 3176, Ruston, LA 71272, USA.
E-mail address: mqiao@latech.edu (M. Qiao).

https://doi.org/10.1016/j.humov.2019.102525
Received 23 November 2018; Received in revised form 23 September 2019; Accepted 23 September 2019
Available online 13 November 2019
0167-9457/

mediolateral (ML) motion prescribed using optical flow (Franz, Francis, Allen, & Thelen, 2016; Qiao, Truong, & Franz, 2018). The intuitive interpretation of those findings is that such entrainment may act to minimize errors between the visual perception of motion and the actual motion of the head and trunk, thereby unifying visual with vestibular and somatosensory feedback (Peterka, 2002; Peterka & Loughlin, 2004). However, we currently lack direct evidence that minimizing these "visual errors" is a control goal for head and trunk stabilization during human walking.

Head and trunk stabilization is critical for regulating walking balance. Usually thought of as arising from corrective motor responses governed by vestibular feedback, this process is more likely governed by the integration of sensory cues from both visual and vestibular feedback (Logan et al., 2010). For example, while vestibular feedback provides a spatial reference for effective head and trunk stabilization during walking (Wilkie, Kountouriotis, Merat, & Wann, 2010), such stabilizing also provides a reliable visual reference for regulating foot placement, navigating complex environments, and avoiding obstacles (Hayhoe, Gillam, Chajka, & Vecellio, 2009; Patla, 1998; Wilkie et al., 2010). In addition, postural deviations that occur normally in walking influence not only the spatial reference for head and trunk stabilization but also optical flow – the visual perception of self-motion, the relative motion of objects in our environment, or both (Kiemel, Zhang, & Jeka, 2011; Logan et al., 2010). Indeed, Logan et al. (2010) nicely summarized available evidence that visual feedback, and optical flow, in particular, can play an important role in both postural stability and navigation during walking. However, it remains unclear how this visual perception of self-motion, in concert with cues from other sensory modalities, is integrated to stabilize the head and trunk during walking – knowledge with particular relevance to navigating unstable environments that could challenge walking balance.

In the neural control of movement, sensory errors arise when actual sensory feedback cues differ from those anticipated to follow from a given motor command (Tseng, Diedrichsen, Krakauer, Shadmehr, & Bastian, 2007; Wolpert & Miall, 1996). Also, on-line monitoring of sensory errors can independently drive motor corrections, for example, decreasing the difference between the visual perception of movement and actual movement of the limb during an arm reaching task (Tseng et al., 2007). Different from the optical flow perturbations used to study entrainment, error-augmentation is tied to the subjects' own performance and is thus more analogous to a biofeedback paradigm**.** In walking, a similar process of error minimization could provide a logical explanation for why people synchronize (i.e., entrain) their head and trunk movements to even very complex mediolateral optical flow oscillations (Franz et al., 2016; Terry, Sinitski, Dingwell, & Wilken, 2012; Warren, Kay, & Yilmaz, 1996). Specifically, the onset of such oscillations, for example in the context of optical flow perturbation studies (Franz et al., 2016; Sinitksi, Terry, Wilken, & Dingwell, 2012), introduces errors between the visual perception of self-motion and the actual motion of the head and trunk. Indeed, we previously proposed that the synchronization of motor responses to visual stimuli during walking is goal-directed, alluding to a process of error minimization wherein proprioceptive and vestibular cues become more consistent with perceived mediolateral motion (Franz et al., 2016; Terry et al., 2012). However, while pseudorandom optical flow perturbations can elicit visuomotor entrainment, they are poorly equipped to provide mechanistic insight into its origin.

Error-augmentation is a paradigm in which movement errors are measured and augmented from an intended trajectory with the goal of strengthening movement control. Although not yet explicitly applied to the visuomotor control of head and trunk motion in walking (though see (Anson, Rosenberg, Agada, Kiemel, & Jeka, 2013)), the paradigm has a rich history in the sensorimotor control literature, particularly in arm reaching tasks (Patton, Wei, Bajaj, & Scheidt, 2013). Largely pioneered by Patton and colleagues, augmenting (i.e., increasing) sensory errors has been shown to effectively elicit motor adaptation while providing mechanistic insight into the origins of that adaptation (Patton et al., 2013). Regarding the role of vision in governing lateral balance in walking, we presume an overriding task goal in which spatial differences between actual motion of the head and trunk and sensory cues via optical flow are minimized (Cowan & Fortune, 2007; Ros & Biewener, 2016). With error-augmentation, we can systematically manipulate those visual errors in real-time to understand their role in governing head and trunk position and thus stabilization during walking. Moreover, given its effect on motor learning and adaptation in arm reaching tasks (Patton et al., 2013), error-augmentation - here in the context of optical flow - may also recalibrate head and trunk control in walking toward the presence of after-effects following prolonged exposure.

Therefore, the purpose of this study was to investigate the role of visual errors in governing the sensorimotor control of head and trunk position during human walking as a means to explain the acute postural response to optical flow perturbations. We used a closed-loop visuomotor error augmentation task in an immersive virtual environment to introduce errors between the visual perception of self-motion and actual instantaneous motion of the head and trunk. We tested the primary hypothesis that minimization of visual errors, achievable during this task only by way of reduced lateral head and trunk movement, is an important and spontaneous feature governing the visuomotor control of human locomotion. The alternative hypothesis would be that visual feedback overrides other sensory modalities and is itself an independent control parameter in governing head and trunk position. To test this alternative hypothesis, we designed our experimental paradigm to include both positive (i.e., visual perception that amplified instantaneous head and trunk motion) and negative (i.e., visual perception that counteracted instantaneous head and trunk motion) visual feedback gains.

2. Materials and methods

2.1. Subjects

We recruited 12 subjects in this study (8 males, 4 females, age: 24.1 ± 4.7 yrs., body mass: 73.3 ± 13.0 kg; height: 176 ± 9 cm, mean ± standard deviation, S.D.). All subjects were healthy without any current neuromusculoskeletal disorders or injuries. Each subject provided written informed consent according to the approved protocol with the Biomedical Sciences Institutional Review Board of the University of North Carolina at Chapel Hill.

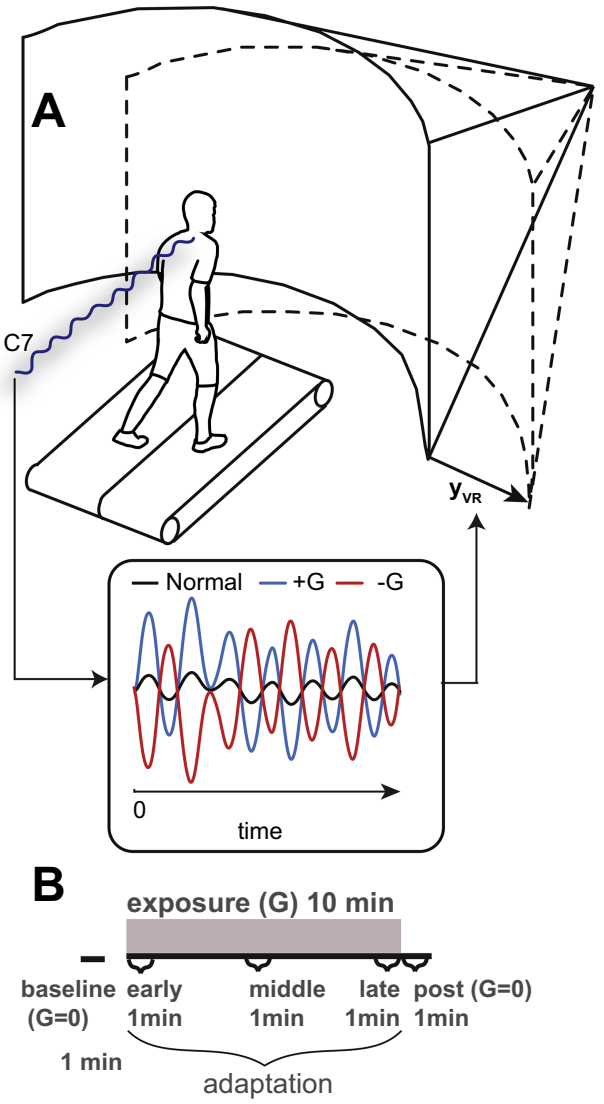

Fig. 1. (A) Subjects walked on a treadmill while watching an immersive virtual hallway with the continuous optical flow while motion capture monitoring the instantaneous position of a 7th cervical vertebrae (C7) marker. Using a real-time controller, the mediolateral position of the projected hallway was prescribed to match that instantaneous C7 position in the mediolateral direction. In some trials, visual errors were introduced by augmenting the mediolateral virtual hallway position by a factor, *G*, defined as the visual gain between the visual perception of trunk motion and the actual motion of the trunk, which took values of ± 2.5 and ± 5.0. (B) Subjects first completed one 3-minute trial at their PWS with zero gain ("Baseline," G = 0). For each of these four gains, our experimental protocol started with zero gain of 15 s to acclimate treadmill walking at zero gain (i.e., normal optical flow, G = 0) and followed by 10 min of exposure (i.e., adaptation) to error-augmented optical flow and finally by 1 min after cessation of error-augmented optical flow (G = 0). We extracted outcome measures from the first ("early"), fifth ("middle"), and tenth ("late") minute of walking with the error-augmented optical flow for analysis.

2.1.1. Experimental protocol and data collection

We first used a photocell timing system (Brower Timing Systems, Draper, UT) to measure subjects' preferred overground walking speed (PWS) from the average of three durations taken to traverse the middle 2 m of a 10 m walkway at their normal, comfortable walking speed (1.36 ± 0.14 $m \cdot s^{-1}$). We established subjects' PWS using an overground walking paradigm, which may yield a different speed than that using a treadmill walking paradigm. All subjects then walked at their PWS on an instrumented split-belt treadmill (1.45 m long × 0.60 m wide belts, Bertec Corp., Columbus, OH). For all treadmill walking trials, subjects watched a speed-matched, immersive virtual hallway rear-projected onto a semi-circular screen (1.45 m radius × 2.54 m height, Fig. 1) surrounding the treadmill (Qiao, Truong, & Franz, 2018). We placed 30 retroreflective markers, including those on anatomical landmarks and marker clusters, on subjects' 7th cervical vertebra (C7), pelvis, and right and left foot, shank, and thigh. A 3D motion capture system (Motion Analysis Corp., Santa Rosa, CA, 10 cameras) recorded the trajectories of each marker at 100 Hz. We chose the mediolateral position of the C7 marker for the feedback control loop of our virtual hallway because C7 is the highest point on the body with large translation

while not affected by head orientation.

We augmented mediolateral optical flow in our virtual environment in real-time based on instantaneous measurements of subjects' trunk position as follows. The mediolateral position of the C7 marker was streamed from the motion capture system through local Ethernet to another computer and received using a Simulink® real-time controller. The midline of the virtual hallway was set for all subjects as the middle of the treadmill, with mediolateral variations prescribed to match the C7 marker trajectory. Specifically, the end of the hallway always remained relatively stationary, while the foreground moved according to this feedback paradigm, thereby emulating head and trunk position changes from one step to the next rather than heading corrections. In some trials, the mediolateral position of the virtual hallway was augmented by a factor (G) times the instantaneous mediolateral C7 position, thereby introducing an error between the visual perception of self-motion and the actual motion of the head and trunk (Fig. 1). G is thereby considered the gain defining the visual error magnitude which, in different trials, took four values (i.e., ± 2.5, ± 5.0). The 5.0 magnitude gain was determined in pilot testing to be the largest possible while ensuring that the virtual hallway remained on the projection screen. Positive/negative gains indicate virtual hallway mediolateral motion was in the same/opposite direction of the instantaneous mediolateral C7 motion, respectively. The feedback delay between the C7 marker position and resulting changes to virtual hallway measured ~14 ms using the available Software Development Toolkit (Motion Analysis Corp.). We provided subjects with verbal instruction only to "walk on the treadmill while watching the hallway" to record naturally emergent patterns in response to error-augmented optical flow.

Subjects first completed one 3-minute trial at their PWS with zero gain ("Baseline," Fig. 1). Subjects then completed four 11-minute walking trials in fully randomized order that incorporated error-augmented optical flow (i.e., "adaptation"). Each of those walking trials consisted of 10 min in the presence of an error augmentation gain on optical flow followed by 1 min of walking with zero gain (i.e., "Post-adaptation"). At the beginning of each 11-min trial, subjects walked for 15 s with fixed optical flow to reach a steady state walking pattern on the treadmill.

2.1.2. Data analysis

We used C7 marker as a surrogate for the trunk motion that is insensitive to the head turns (McAndrew, Dingwell, & Wilken, 2010). We filtered the C7 marker's trajectories using a 4th-order zero-lag low-pass digital Butterworth filter with a cutoff frequency of 8 Hz. Dependent variables for head and trunk position included the step-to-step range of mediolateral trunk motion (intra-step measure, Fig. 4), and the root means square (RMS) of mediolateral trunk position (inter-step measure, Fig. 5). We also calculated time series of step length and step width to resolve step-to-step adjustments in foot placement (Zeni Jr., Richards, & Higginson, 2008). Specifically, we calculated step lengths as the relative anterior-posterior position of consecutive heel markers at heel strike plus the treadmill belt translation during that step. We calculated step widths as the mediolateral distance between consecutive heel positions at heel strike (Qiao, Feld, & Franz, 2018). From their time series, we calculated mean step length and step width and their respective variabilities – the latter reported as the standard deviation (Table 1).

2.2. Statistical analysis

First, we used pairwise t-tests to compare dependent variables from the last minute of the 3-min baseline walking trial to those extracted from walking with error-augmented optical flow (min 1 ["Early"], min 5 ["Middle"], min 10 ["Late"] in adaptation), including after-effects from so. For any pairwise comparison in the texts, we reported effect size as Cohen's d. Second, we used two, 2-

Table 1
The effects of error-augmented optical flow on foot placement kinematics (cm).

		Positive Feedback Gains (G^+)		Negative Feedback Gains (G^-)	
		5.0	2.5	5.0	2.5
SW (14.8 ± 3.8)	Early	15.0 ± 5.2	15.1 ± 5.6	15.3 ± 5.0	15.3 ± 5.2
	Middle	14.6 ± 4.6	14.0 ± 4.5	13.7 ± 4.5	13.7 ± 4.2
	Late	14.6 ± 5.3	14.5 ± 5.8	14.1 ± 4.9	13.9 ± 4.5
	post	12.1 ± 3.9*	13.1 ± 4.7*	15.4 ± 4.9	14.5 ± 5.1
SL (70.5 ± 6.3)	Early	70.3 ± 7.1	70.3 ± 6.8	70.1 ± 6.8	69.5 ± 5.7
	Middle	70.6 ± 7.2	71.0 ± 6.7	71.0 ± 6.7	70.9 ± 6.6
	Late	70.7 ± 7.1	71.4 ± 6.5	70.9 ± 6.7	71.1 ± 6.8
	post	71.6 ± 6.9*	71.8 ± 6.9*	70.3 ± 6.7	70.8 ± 6.8
SWV (2.3 ± 0.6)	Early	2.7 ± 0.7	2.5 ± 0.5	2.9 ± 0.9	2.5 ± 0.6
	Middle	2.9 ± 0.9*	2.7 ± 0.6*	2.9 ± 0.8*	2.5 ± 0.9
	Late	3.0 ± 0.9*	2.8 ± 1.1*	3.0 ± 0.8*	2.7 ± 0.9
	post	2.6 ± 0.7	2.5 ± 0.7	2.4 ± 0.6	2.5 ± 0.9
SLV (2.1 ± 0.6)	Early	2.2 ± 0.7	2.1 ± 0.7	2.2 ± 0.5	2.1 ± 0.7
	Middle	2.1 ± 0.4	1.8 ± 0.5	2.0 ± 0.5	1.9 ± 0.6
	Late	2.1 ± 0.6	2.1 ± 1.0	1.9 ± 0.5	2.0 ± 0.6
	post	1.9 ± 0.5	1.9 ± 0.7	2.0 ± 0.6	1.9 ± 0.7

Data are mean ± standard deviation. SW: step width, SL: step length, SWV: step width variability, SLV: step length variability. Baseline values from normal walking shown in the parentheses. Asterisks (*) indicate significantly different ($p < .05$) from baseline walking.

way repeated measure ANOVAs to determine the effects of and interactions between Magnitude (i.e., 2.5, 5.0) and Phase (i.e., min 1 - "Early", min 5 - "Middle", and min 10 - "Late") for error-augmented optical flow with: (*i*) positive and (*ii*) negative feedback gains including the effect size (η^2) (Keppel & Wickens, 2004). When a significant main effect or interaction was found, we performed *post-hoc* pairwise comparisons to identify which conditions produced those effects. We used a Bonferroni adjusted level of significant for post-hoc pairwise comparisons with a critical alpha level of 0.0085. In addition, the three tests conducted within each 2-way repeated measure ANOVA may cause alpha inflation. We mitigated this problem using two procedures: (*i*) we used the sequential Bonferroni (seqB) correction procedure to control the familywise error rate (FWER) by evaluating each null hypothesis against an α level adjusted to control for the inflated probability of a Type I error (Cramer et al., 2016); (*ii*) we used the Benjamini-Hochberg (BH) procedure to control the false discovery rate (FDR, Type II error). All statistics were coded in MATLAB (R2017a, MathWorks Inc., Natick, MA). We summarize the results of these procedures in Appendix Tables A and B.

3. Results

3.1. The effects of error-augmented optical flow on trunk motion

Mediolateral trunk motion from individual subjects during their initial response to error-augmented optical flow compared to Baseline walking is summarized in Fig. 2, with stride-average profiles shown in Fig. 3. Neither intra- (p-values $>$ .066, Fig. 4) nor inter-step (p-values $>$ .162, Fig. 5) measures of mediolateral trunk motion magnitude decreased in the presence of error-augmented optical flow. Rather, compared to baseline, positive visual errors increased the RMS of mediolateral trunk position (early vs. baseline; G = +2.5: $F(1, 11) = 10.27$, $p = .008$, Cohen's $d = 0.73$, G = +5.0: $F(1, 11) = 7.90$, $p = .017$, $d = 1.02$, Fig. 5A). Moreover, this effect on our inter-step measure of trunk motion scaled in proportion to feedback gain magnitude (main effect, $p = .056$). The intra-step measure, step-to-step mediolateral trunk range of motion magnitude, was unaffected by the presence of error-augmented optical flow with positive gains (early vs. baseline; G = +2.5: $F(1, 11) = 0.07$, $p = .803$, $d = -0.03$, G = +5.0: $F(1, 11) = 1.05$, $p = .327$, $d = -0.15$, Fig. 4A). These early responses to error-augmented optical flow with positive feedback gains were relatively stable; we found no significant phase effects on step-to-step mediolateral trunk range of motion ($F(2, 22) = 0.16$, $p = .854$, $\eta^2 = 0.01$, Fig. 4A) nor the RMS of mediolateral trunk position ($F(2, 22) = 1.29$, $p = .294$, $\eta^2 = 0.11$, Fig. 5A).

Compared to baseline, negative visual errors had no effect on intra-step (early vs. baseline; G = −2.5: $F(1, 11) = 0.32$, $p = .586$, Cohen's $d = -0.07$, G = −5.0: $F(1, 11) = 0.15$, $p = .704$, $d = 0.05$, Fig. 4B) nor inter-step (Fig. 5B, early vs. baseline, $F(1, 11) = 0.77$, $p = .399$, $d = -0.23$, G = −2.5, $F(1, 11) = 0.49$, $p = .500$, $d = 0.13$, G = −5.0) measure of mediolateral trunk motion. In addition, we found no main effect of time (i.e., phase) on either outcome measure (p-*values* $>$ .125, Fig. 4B, Fig. 5B).

Following the 'release' of error-augmented optical flow with positive feedback gains, the RMS of mediolateral trunk motion returned to baseline values within one minute (Fig. 5A). However, despite no apparent phase effects during exposure, step-to-step mediolateral trunk range of motion, our intra-step measure, decreased significantly in Post compared to baseline walking (−12% for G = +5.0, $F(1, 11) = 17.72$, $p = .002$, $d = -0.35$, Fig. 4A; −10% for G = −2.5, $F(1, 11) = 5.57$, $p = .038$, $d = -0.28$, Fig. 4B).

3.2. The effects of error-augmented optical flow on foot placement kinematics

Compared to baseline, we found no significant immediate effect of error-augmented optical flow on step length, step width, nor their variabilities (early vs. baseline, p-values $>$ .063, Table 1). We also found no significant effect of gain magnitude on foot placement kinematics (p-values ≥ .056, Table 1). In contrast, we did find time-dependent changes during prolonged exposure to error-augmented optical flow that was more pronounced for negative than positive visual errors. Specifically, step width ($F(2, 22) = 15.3$, $p_{phase} = 0.002$, $\eta^2 = 0.58$) and step length variability ($F(2, 22) = 8.42$, $p_{phase} = 0.014$, $\eta^2 = 0.43$) decreased significantly with exposure to negative but not positive gains (Table 1). In contrast, step length increased for both positive ($F(2, 22) = 5.37$, $p_{phase} = 0.041$, $\eta^2 = 0.33$) and negative ($F(2, 22) = 27.11$, $p_{phase} < 0.001$, $\eta^2 = 0.71$) gains during exposure. Finally, following "release" of error-augmented optical flow, after-effects in trunk motion were accompanied by significantly longer ($F(1, 11) = 7.07$, $p = .02$, $d = 0.17$) and narrower ($F(1, 11) = 25.08$, $p < .001$, $d = -0.71$) steps than baseline, but only following walking with positive gains (Table 1).

4. Discussion

The primary outcome of this study is that humans appear not to spontaneously minimize visual errors, or those between the visual perception of movement and actual movement of the trunk, during walking. Our results are instead more consistent with our alternative hypothesis – that visual feedback can override other sensory modalities and independently compel adjustments in head and trunk position. We also found little evidence that head and trunk kinematics exhibit time-dependent adaptation during prolonged exposure to error-augmented optical flow in young adults. However, aftereffects do allude to a recalibration of head and trunk stabilization toward more tightly regulated postural control following prolonged exposure to error-augmented optical flow.

4.1. Effects of error-augmented optical flow: exposure versus normal walking

The effects of error-augmented optical flow differed fundamentally from those due to pseudorandom optical flow perturbations, which are more commonly used in the study of balance in walking (Qiao, Truong, & Franz, 2018; Sinitksi et al., 2012). For example,

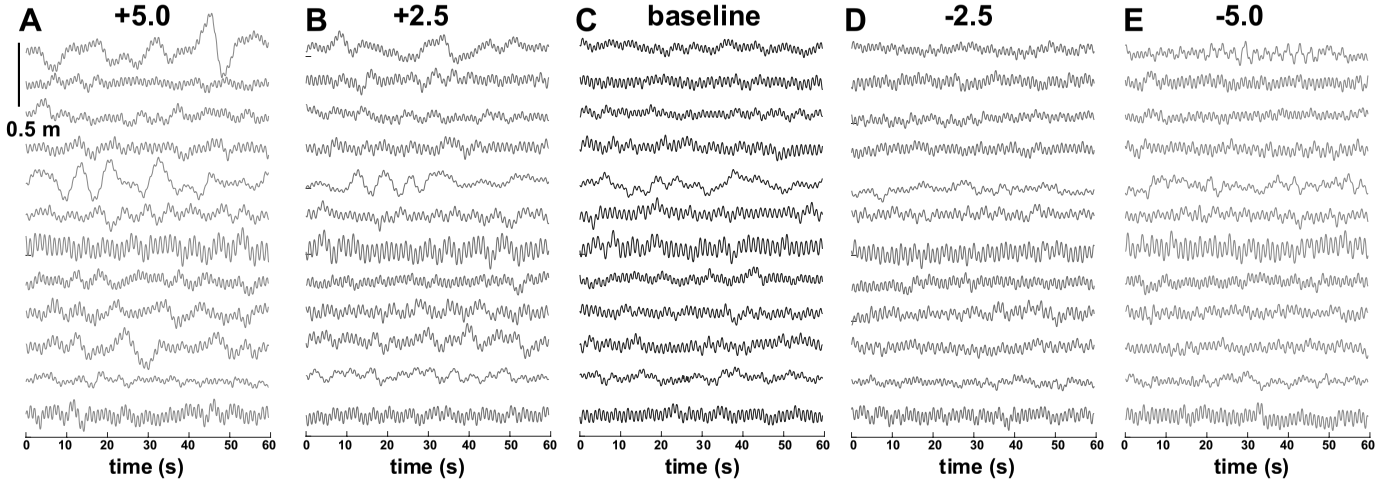

Fig. 2. The medio-lateral position of the trunk (C7 marker) during early exposure for visual gains of (A) G = +5.0, (B) G = +2.5 gain, (D) G = -2.5, and (E) G = -5.0 compared to (C) baseline walking (G = 0) for each subject.

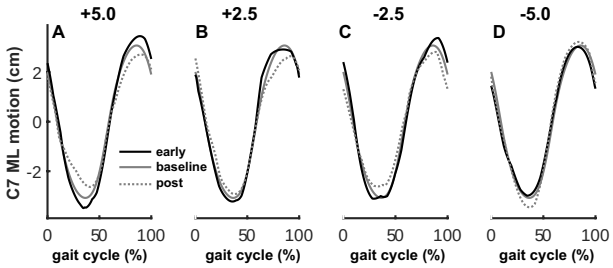

Fig. 3. Stride-averaged mediolateral (ML) C7 position during baseline walking (solid gray line) compared to early exposure (black solid line) and after-effects following cessation of error-augmented optical flow (gray dotted line, i.e., post) for visual gains of (A) G = +5.0, (B) G = +2.5, (C) G = −2.5, and (D) G = −5.0. Each curve was first averaged across all steps taken in that respective phase and then averaged across all subjects. Zero on the ordinate refers to the midline of the treadmill.

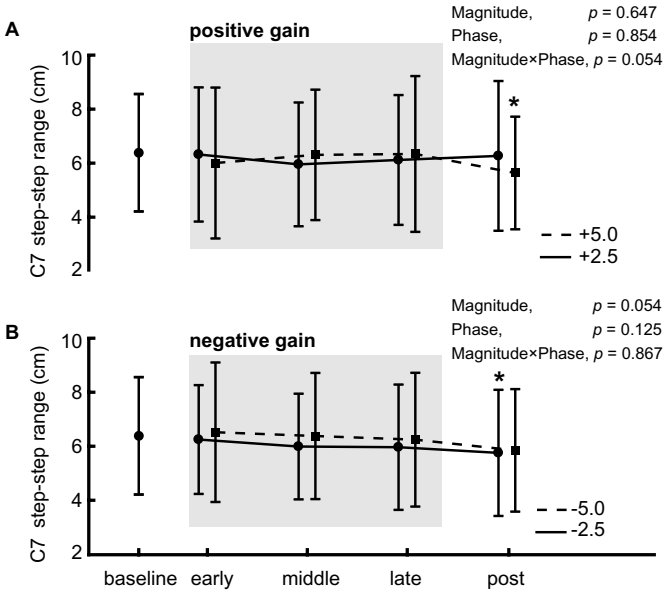

Fig. 4. Our intra-step outcome measure quantifying head and trunk motion during walking. The figure shows the group average (standard deviation) range of step-to-step mediolateral trunk position at different phases (early, middle, and late) of exposure to error-augmented optical flow with (A) positive and (B) negative visual gains compared to baseline walking and after-effects following cessation (post). Asterisks (*) indicate significant ($p < .05$) difference compared to baseline walking. We include the main effects and interaction terms from the repeated measures ANOVA during exposure. The corresponding F values and effect sizes (η^2) for these statistical comparisons follow: $F_{mag}(1,11) = 0.22$, $\eta^2_{mag} = 0.02$; $F_{phase}(2,22) = 0.16$, $\eta^2_{phase} = 0.01$; $F_{mag*phase}(2,22) = 3.34$, $\eta^2_{mag*phase} = 0.23$ in panel A. $F_{mag}(1,11) = 4.64$, $\eta^2_{mag} = 0.30$; $F_{phase}(2,22) = 2.29$, $\eta^2_{phase} = 0.17$; $F_{mag*phase}(2,22) = 0.14$, $\eta^2_{mag*phase} = 0.01$ in panel B.

compared to normal, unperturbed walking, optical flow perturbations can elicit two- to four-fold increases in foot placement variability (Qiao, Truong, & Franz, 2018) and completely decorrelate the step-to-step structure of step width (Dingwell & Cusumano, 2010). In contrast, error-augmented optical flow elicited only subtle changes in foot placement variability. This suggests that lateral balance control in walking is uniquely susceptible to perturbations designed to enhance the visual perception of lateral instability, and not merely to generalized errors in the visual perception of self-motion. Nevertheless, visuomotor control in walking is inherently closed-loop, and error-augmented optical flow affected that control during exposure in ways that inform our broader understanding of walking balance and response to perturbations.

The young adults in our study were unable to, or at least did not, maintain their mediolateral trunk motion near the middle of the treadmill walking surface following exposure to error-augmented optical flow. Our optical flow paradigm used the treadmill's midline as a reference for prescribing visual errors. Specifically, we augmented the visual perception of mediolateral motion as subjects deviated from the treadmill midline, first due to mediolateral trunk oscillations and then further due to changes in average trunk position. Accordingly, in response to positive feedback gains that would act to “push” them away from the treadmill midline, most individual subject trunk trajectories showed low-frequency drift, each corrected throughout several steps, which was not apparent during normal walking (Fig. 2). These “corrections” toward the treadmill midline may be explained by subjects realizing and responding to the physical bounds set by the width of the walking surface. Ultimately, those dynamics likely underlie the increased RMS of mediolateral trunk motion measured in response to positive feedback gains.

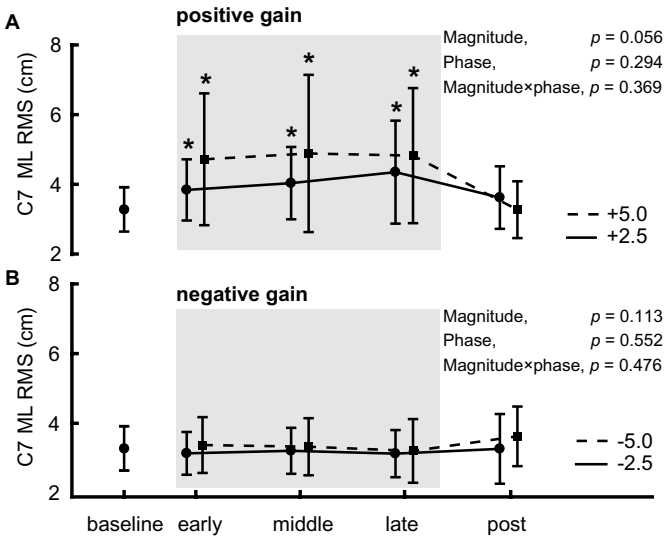

Fig. 5. Our inter-step outcome measure quantifying head and trunk motion during walking. The figure shows the group average (standard deviation) root mean square (RMS) of mediolateral (ML) trunk position at different phase (early, middle, and late) of exposure to error-augmented optical flow with (A) positive and (B) negative visual gains compared to baseline walking and after-effects following cessation (post). Asterisks (*) indicate significant ($p < .05$) difference compared to the baseline. We include the main effects and interaction terms from the repeated measures ANOVA during exposure. The corresponding F values and effect sizes (η^2) for these statistical comparisons follow: $F_{mag}(1,11) = 4.56$, $\eta^2_{mag} = 0.29$; $F_{phase}(2,22) = 1.29$, $\eta^2_{phase} = 0.11$; $F_{mag*phase}(2,22) = 1.04$, $\eta^2_{mag*phase} = 0.09$ in panel A. $F_{mag}(1,11) = 2.97$, $\eta^2_{mag} = 0.21$; $F_{phase}(2,22) = 0.61$, $\eta^2_{phase} = 0.05$; $F_{mag*phase}(2,22) = 0.77$, $\eta^2_{mag*phase} = 0.07$ in panel B.

There are other possible explanations why error-augmented optical flow with positive gains, but not negative gains, increased the excursion (i.e., RMS) of mediolateral trunk position. During walking, humans can distinguish the direction to which they are walking (i.e., their heading) from the direction at which they are looking (e.g., a fixed object in their environment) (Warren & Hannon, 1988). When walking down a hallway, humans may rely on the fixed position of walls in their periphery as an anchored reference for head and trunk stabilization. In the presence of positive visual errors, postural deviations to the right would move that anchored reference of the wall to the right by an amount proportional to feedback gain magnitude. In this example, only by continuing to move to the right would subjects preserve the same relative distance to the anchored reference. This behavior could form a positive feedback loop that would continue to "pull" the body toward the right sidewall of our virtual hallway, an influence that would be altogether absent in the presence of negative visual errors. Therefore, we posit that an anchored visual reference, in our case the walls of the virtual hallway, provide additional spatial information for visuomotor control that is leveraged for head and trunk stabilization.

4.2. Effects of error-augmented optical flow: prolonged exposure and after-effects

Based on prior evidence that subjects adapt to pseudorandom optical flow perturbations (Thompson & Franz, 2017), we hypothesized that our outcome measures would exhibit tuning via time-dependent changes with prolonged exposure. Our data did not fully support this hypothesis. Subjects' behavioral response to error-augmented optical flow was relatively invariant across the duration of each trial. Some evidence suggests that humans adapt their step-to-step control of step width to regulate mediolateral motion of the trunk (Hurt, Rosenblatt, Crenshaw, & Grabiner, 2010), measured here via the C7 marker. This may explain why we observed time-dependent changes in SWV but relatively well-preserved trunk kinematics. Also, time-dependent effects on step width and step length variability, apparent in response to negative gains, were inconsistent across the two amplitudes. Compared to those following the onset of optical flow perturbations, initial effects were generally smaller in response to the present paradigm. In light of these smaller effects, one interpretation is that there was less need for or benefit to adapting to error augmented optical flow during each 10-min trial. However, we suspect that some adaptation did occur; as hypothesized, prolonged exposure to error-augmented optical flow elicited aftereffects that persisted following "release" of error-augmented optical flow. Most notably, these aftereffects included longer, narrower steps, and smaller step-to-step mediolateral trunk range of motion, particularly following exposure to larger amplitude positive feedback gains. Here, we see "release" of error-augmented optical flow as analogous to catch trials in arm reaching paradigms that use error-augmentation. Specifically, the cessation of error-augmentation is generally designed to reveal changes in the underlying strategies used to control movement. Accordingly, we interpret the measured aftereffects in our study to suggest that head and trunk stabilization had become more tightly regulated following exposure compared to baseline. Such an outcome would be anticipated if error-augmented optical flow with positive gains increased the demands placed on the postural control system, presumably to maintain head and trunk position near the midline of the treadmill with smaller mediolateral oscillations.

That subjects exhibited at least temporary reductions in step-to-step postural sway after exposure to error-augmented optical flow

may have translational implications. Most falls occur during locomotor activities such as walking, during which preserving the body's center of mass within the mediolateral base of support is important for balance integrity. Accordingly, individuals with excessive mediolateral postural sway may be at a greater risk of lateral instability and falls (Hilliard et al., 2008). Some evidence suggests that visual feedback can facilitate improved motor learning with beneficial effects. However, it is unclear what type of optical flow paradigm is the best (Peterson, Rios, & Ferris, 2018). Balance perturbations, for example via mediolateral optical flow oscillations, provide the opportunity to practice reactive adjustments with promising effects on balance control (Richards et al., 2019) and reducing falls risk (Grabiner, Bareither, Gatts, Marone, & Troy, 2012). Conversely, error-augmented optical flow with positive feedback gains may lead to more tightly regulated postural control following exposure. Because perturbations and error augmentation via optical flow represent fundamentally different paradigms for balance training, thereby differing in their elicited responses and aftereffects, specific recommendations for clinical translation are challenging. The advent and more widespread adoption of wearable and low-cost virtual reality technology should inspire continued research toward determining which optical flow paradigms, or combinations thereof, can provide the most beneficial effect on balance integrity, for example in older adults at high risk of falling.

4.3. Limitations

Foremost, although we discuss the implications of our outcomes for balance control in people with walking balance deficits or those at risk of falls, this study focused on otherwise healthy young subjects. Accordingly, our results may not generalize to those populations in the way we predict. In addition, for practical considerations in our study design, we opted for 10-min trials. The response to longer exposure to error-augmented optical flow, like what we might expect from a training paradigm, are difficult to anticipate. The C7 marker provides a surrogate representation of trunk translation. Future work may consider the complexities of head rotation together with trunk translation. We also constrained treadmill walking speed, and the response to error-augmented optical flow may have differed if subjects were allowed to regulate their walking speed throughout each trial like when navigating real-world environments. Finally, after-effects reported herein allude to changes in neuromuscular control that our experimental design was not equipped to fully capture. Future studies involving electromyographic recordings, particularly of postural control muscles, may provide important insight into those changes in control.

5. Conclusions

To our knowledge, this is the first study to apply an error-augmentation paradigm to understand the role of visual errors in governing head and trunk stabilization during walking. In contrast to our earlier explanation for the mechanism governing visuomotor entrainment to optical flow perturbations, young subjects in our study did not respond consistently to minimize the errors between visual perception of movement and actual movement of the head and trunk. Thus, we cannot conclude that unifying visual with vestibular and somatosensory feedback is always a universal control goal in human walking, at least in the context of head and trunk stabilization. Rather, visual feedback appears to override other sensory modalities and independently compel adjustments in head and trunk position. Finally, our results also have important translational implications. Although we focused on young adults, aftereffects in the form of reduced mediolateral postural sway evident in our data may have important implications for the use of error-augmented optical flow to enhance the integrity of walking balance control through training, for example in older adults.

Acknowledgments

Funded by a grant from NIH (R56AG054797).

Appendix A. Appendix

Table A
Results from the sequential Bonferroni (seqB) and Benjamini-Hochberg (BH) procedures for the data in Table 1.

	Effect	Positive feedback gains (G^+)					Negative feedback gains (G^-)				
		p value	α_{adj} seqB	α_{adj} BH	H_0 seqB	H_0 BH	p value	α_{adj} seqB	α_{adj} BH	H_0 seqB	H_0 BH
SW	M	0.513	0.0500	0.0500	Retained	Retained	0.875	0.0500	0.0500	Retained	Retained
	P	0.229	0.0250	0.0333	Retained	Retained	0.002	0.0167	0.0167	Rejected	Rejected
	M × P	0.227	0.0167	0.0167	Retained	Retained	0.875	0.0250	0.0333	Retained	Retained
SL	M	0.248	0.0500	0.0500	Retained	Retained	0.534	0.0500	0.0500	Retained	Retained
	P	0.041	0.0167	0.0167	Retained	Retained	< 0.001	0.0167	0.0167	Rejected	Rejected
	M × P	0.092	0.0250	0.0333	Retained	Retained	0.495	0.0250	0.0333	Retained	Retained
SWV	M	0.135	0.0167	0.0167	Retained	Retained	0.056	0.0167	0.0167	Retained	Retained
	P	0.495	0.0250	0.0333	Retained	Retained	0.325	0.0250	0.0333	Retained	Retained
	M × P	0.927	0.0500	0.0500	Retained	Retained	0.982	0.0500	0.0500	Retained	Retained

(*continued on next page*)

Table A (*continued*)

	Effect	Positive feedback gains (G^+)					Negative feedback gains (G^-)				
		p value	α_{adj} seqB	α_{adj} BH	H_0 seqB	H_0 BH	*p* value	α_{adj} seqB	α_{adj} BH	H_0 seqB	H_0 BH
SLV	M	0.339	0.0500	0.0500	Retained	Retained	0.744	0.0500	0.0500	Retained	Retained
	P	0.128	0.0167	0.0167	Retained	Retained	0.014	0.0167	0.0167	Rejected	Rejected
	M × P	0.160	0.0250	0.0333	Retained	Retained	0.653	0.0250	0.0333	Retained	Retained

SW: step width, SL: step length, SWV: step width variability, SLV: step length variability. M: magnitude, P: Phase, M × P: the interaction between Magnitude and Phase. α_{adj} seqB = the adjusted alpha level with the sequential Bonferroni procedure; α_{adj} BH = the adjusted alpha level with the Benjamini-Hochberg procedure; H_0 seqB = evaluation of the null hypotheses with the sequential Bonferroni procedure; H_0 BH = evaluation of the null hypotheses with the Benjamini-Hochberg procedure.

Table B
Results from the sequential Bonferroni (seqB) and Benjamini-Hochberg (BH) procedures for the data in Figs. 4 and 5.

	Effect	Positive feedback gains (G^+)					Negative feedback gains (G^-)				
		p value	α_{adj} seqB	α_{adj} BH	H_0 seqB	H_0 BH	*p* value	α_{adj} seqB	α_{adj} BH	H_0 seqB	H_0 BH
C7	M	0.647	0.0250	0.0333	Retained	Retained	0.054	0.0167	0.0167	Retained	Retained
Step-step	P	0.854	0.0500	0.0500	Retained	Retained	0.125	0.0250	0.0333	Retained	Retained
range	M × P	0.054	0.0167	0.0167	Retained	Retained	0.867	0.0500	0.0500	Retained	Retained
C7	M	0.056	0.0167	0.0167	Retained	Retained	0.113	0.0167	0.0167	Retained	Retained
ML	P	0.294	0.0250	0.0333	Retained	Retained	0.552	0.0500	0.0500	Retained	Retained
RMS	M × P	0.369	0.0500	0.0500	Retained	Retained	0.476	0.0250	0.0333	Retained	Retained

M: magnitude, P: Phase, M × P: the interaction between Magnitude and Phase. α_{adj} seqB = the adjusted alpha level with the sequential Bonferroni procedure; α_{adj} BH = the adjusted alpha level with the Benjamini-Hochberg procedure; H_0 seqB = evaluation of the null hypotheses with the sequential Bonferroni procedure; H_0 BH = evaluation of the null hypotheses with the Benjamini-Hochberg procedure.

References

Anson, E., Rosenberg, R., Agada, P., Kiemel, T., & Jeka, J. (2013). Does visual feedback during walking result in similar improvements in trunk control for young and older healthy adults? *Journal of Neuroengineering and Rehabilitation, 10*, 110.

Cowan, N. J., & Fortune, E. S. (2007). The critical role of locomotion mechanics in decoding sensory systems. *Journal of Neuroscience, 27*, 1123–1128.

Cramer, A. O., van Ravenzwaaij, D., Matzke, D., Steingroever, H., Wetzels, R., Grasman, R. P., & Wagenmakers, E. J. (2016). Hidden multiplicity in exploratory multiway ANOVA: Prevalence and remedies. *Psychonomic Bulletin & Review, 23*, 640–647.

Dingwell, J. B., & Cusumano, J. P. (2010). Re-interpreting detrended fluctuation analyses of stride-to-stride variability in human walking. *Gait & Posture, 32*, 348–353.

Franz, J. R., Francis, C., Allen, M., & Thelen, D. G. (2016). Visuomotor entrainment and the frequency-dependent response of walking balance to perturbations. *IEEE Transactions on Neural Systems and Rehabilitation Engineering, 25*, 1135–1142.

Grabiner, M. D., Bareither, M. L., Gatts, S., Marone, J., & Troy, K. L. (2012). Task-specific training reduces trip-related fall risk in women. *Medicine & Science in Sports & Exercise, 44*, 2410–2414.

Hayhoe, M., Gillam, B., Chajka, K., & Vecellio, E. (2009). The role of binocular vision in walking. *Visual Neuroscience, 26*, 73–80.

Hilliard, M. J., Martinez, K. M., Janssen, I., Edwards, B., Mille, M. L., Zhang, Y., & Rogers, M. W. (2008). Lateral balance factors predict future falls in community-living older adults. *Archives of Physical Medicine and Rehabilitation, 89*, 1708–1713.

Hurt, C. P., Rosenblatt, N., Crenshaw, J. R., & Grabiner, M. D. (2010). Variation in trunk kinematics influences variation in step width during treadmill walking by older and younger adults. *Gait & Posture, 31*, 461–464.

Keppel, G., & Wickens, T. D. (2004). Effect Size, Power, and Sample Size. In *Design and Analysis: a Researcher's Handbook, 4th Edition* (Vol. 5, pp. 159–179). Upper Saddle River, N.J.: Pearson Prentice Hall.

Kiemel, T., Zhang, Y. F., & Jeka, J. J. (2011). Identification of neural feedback for upright stance in humans: stabilization rather than sway minimization. *Journal of Neuroscience, 31*, 15144–15153.

Logan, D., Kiemel, T., Dominici, N., Cappellini, G., Ivanenko, Y., Lacquaniti, F., & Jeka, J. J. (2010). The many roles of vision during walking. *Experimental Brain Research, 206*, 337–350.

McAndrew, P. M., Dingwell, J. B., & Wilken, J. M. (2010). Walking variability during continuous pseudo-random oscillations of the support surface and visual field. *Journal of Biomechanics, 43*, 1470–1475.

O'Connor, S. M., & Kuo, A. D. (2009). Direction-dependent control of balance during walking and standing. *Journal of Neurophysiology, 102*, 1411–1419.

Patla, A. E. (1998). How is human gait controlled by vision? *Ecological Psychology, 10*, 287–302.

Patton, J. L., Wei, Y. J., Bajaj, P., & Scheidt, R. A. (2013). Visuomotor learning enhanced by augmenting instantaneous trajectory error feedback during reaching. *PLoS One, 8*, e46466.

Peterka, R. J. (2002). Sensorimotor integration in human postural control. *Journal of Neurophysiology, 88*, 1097–1118.

Peterka, R. J., & Loughlin, P. J. (2004). Dynamic regulation of sensorimotor integration in human postural control. *Journal of Neurophysiology, 91*, 410–423.

Peterson, S. M., Rios, E., & Ferris, D. P. (2018). Transient visual perturbations boost short-term balance learning in virtual reality by modulating electrocortical activity. *Journal of Neurophysiology, 120*(4), 1998–2010. https://doi.org/10.1152/jn.00292.2018.

Qiao, M., Feld, J. A., & Franz, J. R. (2018). Aging effects on leg joint variability during walking with balance perturbations. *Gait & Posture, 62*, 27–33.

Qiao, M., Truong, K. N., & Franz, J. R. (2018). Does local dynamic stability during unperturbed walking predict the response to balance perturbations? An examination across age and falls history. *Gait & Posture, 62*, 80–85.

Richards, J. T., Selgrade, B. P., Qiao, M., Plummer, P., Wikstrom, E. A., & Franz, J. R. (2019). Time-dependent tuning of balance control and aftereffects following optical flow perturbation training in older adults. *Journal of Neuroengineering and Rehabilitation, 16*, 81.

Ros, I. G., & Biewener, A. A. (2016). Optic flow stabilizes flight in ruby-throated hummingbirds. *Journal of Experimental Biology, 219*, 2443–2448.

Sinitksi, E. H., Terry, K., Wilken, J. M., & Dingwell, J. B. (2012). Effects of perturbation magnitude on dynamic stability when walking in destabilizing environments. *Journal of Biomechanics, 45*, 2084–2091.
Terry, K., Sinitski, E. H., Dingwell, J. B., & Wilken, J. M. (2012). Amplitude effects of medio-lateral mechanical and visual perturbations on gait. *Journal of Biomechanics, 45*, 1979–1986.
Thompson, J. D., & Franz, J. R. (2017). Do kinematic metrics of walking balance adapt to perturbed optical flow? *Human Movement Science, 54*, 34–40.
Tseng, Y. W., Diedrichsen, J., Krakauer, J. W., Shadmehr, R., & Bastian, A. J. (2007). Sensory prediction errors drive cerebellum-dependent adaptation of reaching. *Journal of Neurophysiology, 98*, 54–62.
Warren, W. H., & Hannon, D. J. (1988). Direction of self-motion is perceived from optical-flow. *Nature, 336*, 162–163.
Warren, W. H., Kay, B. A., & Yilmaz, E. H. (1996). Visual control of posture during walking: Functional specificity. *Journal of Experimental Psychology. Human Perception and Performance, 22*, 818–838.
Wilkie, R. M., Kountouriotis, G. K., Merat, N., & Wann, J. P. (2010). Using vision to control locomotion: Looking where you want to go. *Experimental Brain Research, 204*, 539–547.
Wolpert, D. M., & Miall, R. C. (1996). Forward models for physiological motor control. *Neural Networks, 9*, 1265–1279.
Zeni, J. A., Jr., Richards, J. G., & Higginson, J. S. (2008). Two simple methods for determining gait events during treadmill and overground walking using kinematic data. *Gait & Posture, 27*, 710–714.